Four years of structural health monitoring of the San Pietro bell tower in Perugia, Italy: two years before the earthquake versus two years after

Pier Francesco Giordano*

Department of Architecture, Built Environment and Construction Engineering,
Politecnico di Milano,
Piazza Leonardo da Vinci 32, 20133 Milan, Italy
Email: pierfrancesco.giordano@polimi.it
*Corresponding author

Filippo Ubertini, Nicola Cavalagli and Alban Kita

Department of Civil and Environmental Engineering,
University of Perugia,
Via G. Duranti 93, 06125 Perugia, Italy
Email: filippo.ubertini@unipg.it
Email: nicola.cavalagli@unipg.it
Email: alban.kita@unipg.it

Maria Giovanna Masciotta

Department of Civil Engineering,
Campus de Azurém,
University of Minho,
4800-058 Guimarães, Portugal
Email: mg.masciotta@gmail.com

Abstract: This paper addresses the structural health monitoring (SHM) of the bell tower of the Basilica of San Pietro in Perugia, Italy, which is located in a seismic area. Known as one of the landmarks of the Umbrian capital, the tower belongs to a monumental complex of exceptional historical and cultural value. Therefore, its protection with respect to earthquakes is an important issue. To this purpose, a vibration-based SHM system able to detect anomalies in the structural behaviour by means of statistical process control tools has been installed in the tower and is under continuous operation since December 2014. The effects of the 2016–2017 Central Italy seismic sequence were clearly detected by this system, even if earthquakes took place at relatively large distance from the bell tower. The large amount of SHM data collected over four years allowed to assess the modifications in the structural behaviour of the bell tower in post-earthquake conditions.

Keywords: structural health monitoring; SHM; operational modal analysis; OMA; post-earthquake assessment; environmental effects; heritage structures; masonry towers; preservation of architectural heritage; Italy.

Reference to this paper should be made as follows: Giordano, P.F., Ubertini, F., Cavalagli, N., Kita, A. and Masciotta, M.G. (2020) 'Four years of structural health monitoring of the San Pietro bell tower in Perugia, Italy: two years before the earthquake versus two years after', *Int. J. Masonry Research and Innovation*, Vol. 5, No. 4, pp.445–467.

Biographical notes: Pier Francesco Giordano is a PhD student at the Department of Architecture, Built Environment and Construction Engineering (DABC) of Politecnico di Milano, Italy. He received his Master's in Structural Analysis of Monuments and Historical Constructions (SAHC) from University of Minho, Portugal, and Polytechnic University of Catalonia, Spain. He is currently working on the value of information from Bayesian decision theory and structural health monitoring.

Filippo Ubertini is a Full Professor of Structural Design in the University of Perugia where he teaches Advanced Structural Design. He graduated Cum Laude in Civil Engineering in the University of Perugia in 2005. He received his PhD in Civil Engineering from the University of Pavia in 2009. He is a Visiting Scholar from the Columbia University in 2008 and a coordinator of UNIPG RT in two Horizon 2020 projects and of a national PRIN project. He is also an EB member of Shock and Vibration, Mathematical Problems in Engineering and a recipient of prizes and awards.

Nicola Cavalagli currently received his Postdoctoral position at the University of Perugia in Italy. He teaches in the laboratories of Structural Mechanics since 2011 and in Architectural Restoration since 2015. His research interests are mainly focused on the analysis of historical constructions, with special attention to the homogenisation techniques of masonry material and the analysis of masonry arches, vaults and domes, considering geometrical uncertainties effects. His recent studies are devoted to the development of structural health monitoring strategies applied to heritage constructions for their preventive conservation.

Alban Kita is a PhD student at the Department of Civil and Environmental Engineering of University of Perugia, Italy and with a collaboration cotutelle agreement also at the University of Minho, Portugal. Within the framework of vibration-based long-term structural health monitoring methods combined with numerical model-based methods, he is currently working on innovative SHM solutions aimed at earthquake-induced damage detection, localisation and quantification in heritage masonry buildings.

Maria Giovanna Masciotta obtained her dual-degree PhD in 2015 within a joint programme between the University of Minho (Portugal) and the University of 'Gabriele d'Annunzio' of Chieti-Pescara (Italy), being therefore awarded the mention of 'Doctor Europaeus'. Since then, she has been working as a Post-Doc Researcher at the Institute for Sustainability and Innovation in Structural Engineering (ISISE), which is the largest research unit in the field of Structural Engineering in Portugal. Her scientific research activity embraces the areas of inspection and diagnosis, NDT, dynamic testing, operational and experimental modal analyses, numerical modelling, structural health monitoring, damage identification, seismic vulnerability, maintenance and preventive conservation of built cultural heritage, having a track record of publications on these topics in both ISI journals and international conferences.

This paper is a revised and expanded version of a paper entitled 'Diagnostic investigations and structural health state assessment of San Pietro bell tower in Perugia' presented at 10IMC – 10th International Masonry Conference, Milan, Italy, 9–11 July 2018.

1 Introduction

The conservation of structures is a complex activity which requires the acquisition of information on the assets. Knowledge can derive from the analysis of existing documents such as designs and reports or from new in situ surveys and experimental tests. In the case of historic buildings both sources of data are often restricted either because of the lack and incompleteness of documents in archives or because of the impossibility to perform invasive tests that may compromise the integrity of the constructions (Bartoli et al., 2012). In this context, structural health monitoring (SHM) techniques appear to be particularly attractive (Ramos et al., 2010; De Stefano et al., 2016; Gattulli et al., 2016; Lorenzoni et al., 2016; Elyamani et al., 2017; Clementi et al., 2017; Masciotta et al., 2017a). They are based on the continuous observation – by means of sensors – of a physical phenomenon which is related to the health of the structure (Peeters et al., 2001; Worden et al., 2002; Magalhães et al., 2012). Multiple physical phenomena and structural parameters can be considered as well. In this way, the structural conditions are assessed and tracked, and the occurrence of anomalies can be detected. Since the principle of minimum intervention is satisfied when using SHM methods, they are considered adequate for heritage preservation (ICOMOS/ISCARSAH, 2005). Despite the advantages, regular applications of SHM systems on real monuments are still rare (Guidobaldi, 2016). The case of San Pietro bell tower, located in Perugia, Italy, is a remarkable example of long-term vibration-based SHM. The bell tower has been monitored since December 2014 by a team of researchers of the Department of Civil and Environmental Engineering from University of Perugia, which includes the authors of this paper affiliated with the institution (Ubertini et al., 2016). The SHM system identifies and tracks in time the natural frequencies of the monumental tower using an automatic stochastic subspace identification (SSI) procedure and detects anomalies in the global structural behaviour by means of statistical analysis of the natural frequencies. Environmental sensors complete the SHM system and allow studying the influence of environmental parameters on the structural behaviour. The hardware of the SHM system is quite simple and includes three accelerometers placed at the base of the cusp of the bell tower. A similar method has been used on other monumental masonry towers (Saisi et al., 2015; Cabboi et al., 2015; Cavalagli et al., 2017). Accidentally, after almost two years of continuous SHM, a series of earthquakes hit Central Italy. The major seismic events took place in the period from 24th August 2016 to 18th January 2017, with epicentre between 55 and 100 km from Perugia. Structural damages were clearly detected by the SHM system but not from the visual inspection of the monument (Kita et al., 2017; Ubertini et al., 2018; Giordano et al., 2018).

The aim of this paper is to investigate the effects of the aforementioned earthquakes on the structural behaviour of San Pietro bell tower based on SHM results. In addition to this first introductory chapter, the rest of paper is organised as follows. Section 2 concerns the presentation of the bell tower, from the historical, geometric, and material points of view. Section 3 focuses on the SHM system and the damage detection procedure. Section 4 is the core of this work. First, the dynamic response of the bell tower under several seismic excitations is presented. After that, the output of the SHM system is shown and analysed, including the plot of identified natural frequencies over time and the control charts used for damage detection. Five natural frequencies are tracked over more than four years. The aim of the SHM strategy consists in distinguishing the variations in natural frequencies due to exogenous factors, induced by environmental and operational effects, from those induced by endogenous factors, i.e., loss of stiffness in structural elements due to the occurrence of damage. Novelty analysis techniques accomplish this task, based on statistical examination of a damage index, the T^2 statistic, which is displayed in the control chart. The probability distribution of the T^2 statistic in undamaged and damaged conditions is studied. Besides, the correlation analysis between natural frequencies and temperature and between the T^2 statistic and temperature is carried out before and after the seismic events. The last part of Section 4 is dedicated to the ambient vibration test (AVT) carried out on 18th May 2017. The results are compared with those obtained from the AVT performed in 2015 aiming to examine the mode shapes of the tower in pre- and post-earthquake conditions. The study of mode shapes is particularly convenient since they are less sensitive to environmental effects with respect to natural frequencies. Section 5 is focused on the recalibration of the SHM algorithm. Section 6 concludes the paper.

2 San Pietro bell tower

2.1 General overview

The object of this work is the bell tower of the monumental complex of the Basilica of San Pietro, Figure 1, which is located on the Caprario Mount, in the South of the historical centre of Perugia, in Central Italy. The monastery was founded in the year 996, on the former Episcopal Church of the City. At present, it comprises the Basilica, three cloisters, the bell tower and numerous buildings that embody the monastery, the Department of Agricultural Studies, and the seismic observatory entitled to Andrea Bina, pioneer of seismology. From its construction to present days, San Pietro bell tower has experienced a complex history. Numerous structural and aesthetic interventions have transformed the appearance of the monument over time. The exact year of the construction of the bell tower is unknown. Anyway, the earliest document mentioning the tower dates back to 1286. Substantial modifications were carried out at the end of the 14th century, when the religious complex was converted into a fortress. In 1387, the cusp and part of the belfry were demolished, and the whole bell tower was transformed into a defensive structure. A few years later, in 1393, Pope Boniface IX ordered a further lowering of the belfry for military purposes. For more than half a century, the structure remained in that condition.

In 1463, Bernardo Rossellino, a famous Renaissance artist, was commissioned to restore the monument. He redesigned the bell tower in Florentine-gothic style. The works were completed in 1468. Afterwards, the bell tower was repaired several times because of earthquakes and, especially, lightning shocks. The chronicles refer about collapses and damages caused by lightning shocks in the following years: 1481, 1498, 1569, 1574, 1592, 1616, 1618, 1640, 1667, 1674, 1730, 1778, and 1787. Around 1730, metal tie rods were introduced in the structure, at various heights and locations. These elements were replaced several times. In 1753, the shaft was confined with metal strips because of worrying longitudinal cracks. In 1788 one of the first lightning rods was installed on the tower, which proved to be effective. The available sources do not mention any significant structural works during the 19th century.

Figure 1 Evolution of the bell tower, (a) miniature from Register of *Collegio del Cambio*, 1377 (b) fresco in *Priori* Palace, by Benedetto Bonfigli, 1455–1479 (c) painting representing Perugia during the middle age by Gaspar Van Vittel, early 18th century (d) the current aspect of the tower (see online version for colours)

Three important interventions were executed during the last century. The structure which supports the four bells was introduced between the years 1929 and 1933, consisting of a metal scaffolding of 9 m height and 5.5 ton weight that rests on a series of beams penetrating the shaft. It was considered necessary to mitigate the oscillations caused by the swinging of the bells. Nevertheless, the construction turned out to be a rather invasive intervention. It implied the demolition of the vault between the shaft and the belfry. Moreover, the arches that supported the vault were consolidated with concrete insertions. In 1951, consolidation works were carried out in the basement, since signs of crushing had appeared. They consisted of grout injections and infilling of one access door. In addition, the bell tower was damaged by the 1997 Marche-Umbria earthquake and it was restored in 2002. On that occasion, the belfry was strengthened with modern materials, such as carbon and glass fibres.

2.2 Geometric and material survey

The bell tower is 61.4 m high and is conventionally subdivided in four parts, namely: basement, shaft, belfry, and cusp, see Figure 2.

The basement is 8 m high, having the shape of a truncated dodecagonal pyramid. It is characterised by massive stone walls, with thickness ranging roughly from 2 m to 3.5 m. Inside, the space is delimited by a segmental dome of 6 metres in diameter. The external leaves are made of irregular travertine blocks.

The shaft has a dodecagonal cross section and 1.8 m average thickness walls. On the outside, it is divided by belt courses into three sections. The outer leaf is made of limestone blocks and brick insertions. Internally, the structure is rather complex, but it can be subdivided into two spaces. The lower one is a room which is delimited by a segmental dome. The second space starts from a height of 12 m and occupies the remaining volume of the shaft. The entrance door is located at this level. Here, masonry stairs go anticlockwise around the walls of the shaft. The final portion of the staircase was demolished to allow the construction of the metal scaffolding, which stands from the height of 23 m and extends for 9 m up to the belfry. Recently, two timber floors were constructed to allow easy access to the belfry. At the height of 24 m, the remains of the demolished vault are visible. Hereupon, the interior structure of the shaft assumes a hexagonal shape. Regarding materials, the walls are mostly made of limestone, while arches and vaults are made of bricks. Concrete insertions are present as well.

Figure 2 San Pietro bell tower, (a) basement (b) interior of the shaft (c) metal scaffolding supporting the four bells (d) interior of the cusp (see online version for colours)

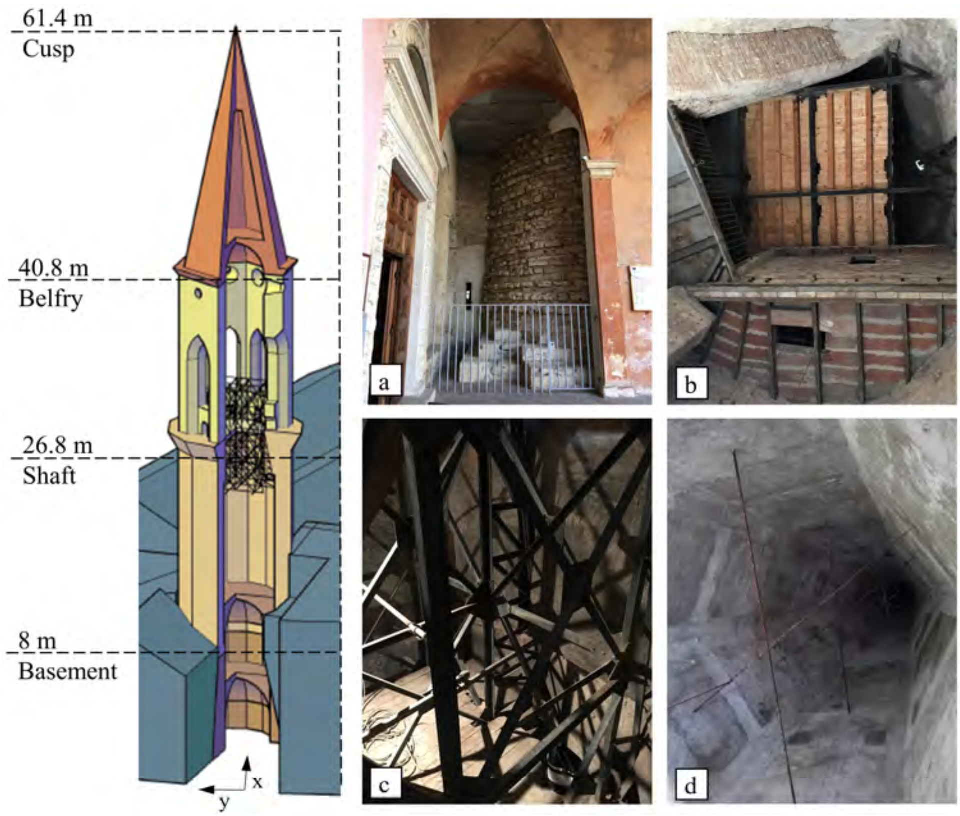

At 26.8 m height, a 0.40 m thick slab separates the shaft from the belfry. The passage between the two bodies is marked by decorative brackets at the exterior. The belfry has a hexagonal shape and extends up to a height of 40.8 m. The thickness of the walls decreases to 1.2 m. The belfry is subdivided in two spaces by a timber floor. The lower portion is pierced by six rectangular openings, while large mullioned windows characterise the upper part. As for the materials, the belfry is mostly made of travertine and brick masonry, whereas the columns of the mullioned windows, capitals and other decorations are in travertine.

A segmental dome completes the belfry and delimits the boundaries of the cusp, which is the terminal element of the bell tower. The cusp has the shape of a hexagonal pyramid. The last 6 metres consist of a solid masonry block. The cusp is mainly made of travertine with an external layer of bricks.

3 SHM procedure

The San Pietro bell tower has been continuously monitored for about four years. The SHM procedure is based on the continuous identification of five natural frequencies and on the statistical analysis of their variation, aiming at distinguishing modifications in the dynamic behaviour of the monument due to exogenous factors, such as temperature, from those induced by endogenous causes, attributable to structural damages. The SHM procedure is formed by a limited number of components and it consists of four main steps, namely:

1 data acquisition

2 data storage

3 data transmission

4 data analysis.

The input data are the horizontal measured accelerations in two perpendicular directions; the output is a control chart used for damage detection. The general framework of the SHM strategy and the sensor layout are displayed in Figure 3.

Figure 3 SHM framework (see online version for colours)

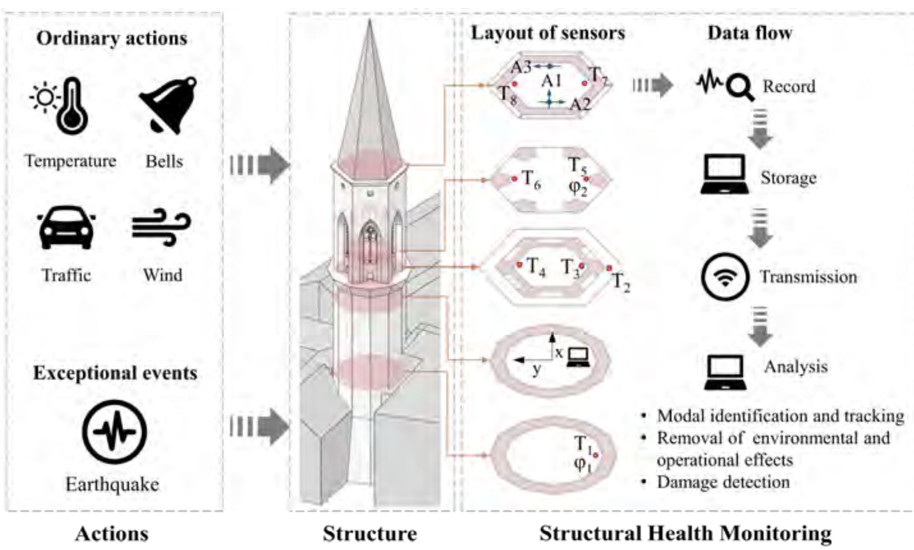

The SHM system comprises three uniaxial piezoelectric accelerometers (model PCB 393B12, 10V/g sensitivity) and a multi-channel data acquisition system (carrier model cDAQ-9184, with NI 9234 data acquisition modules), which are located at the base of the cusp. The acquisition system is connected to a personal computer placed in the shaft, which is used for data acquisition and real-time elaboration. Records from accelerometers are sampled at 100 Hz and stored in progressive files of 30 min for automated modal identification. Then, data are transmitted via internet to a remote server located in the Laboratory of Structural Dynamics of the Department of Civil and Environmental Engineering of the University of Perugia. Here, data are processed through a specific

MATLAB algorithm, which involves the following three phases. First, the automated modal identification and modal tracking processes, which include in turn: a pre-processing analysis to identify and correct anomalies in the data; detection and removal of vibrational data due to the swinging bells; application of a low-pass filter and decimation of data to 40 Hz; application of a fully automated SSI procedure (Ubertini et al., 2013); and modal tracking of the estimated parameters based on a similarity check. Second, removal of environmental effects by means of a combination between the techniques of multiple linear regression (MLR) and principal component analysis (PCA). Finally, novelty analysis procedure for damage detection. The quantities used for damage detection are contained in the residual error matrix, E, defined as:

$$\boldsymbol{E} = \boldsymbol{Y} - \hat{\boldsymbol{Y}} \tag{1}$$

where $\boldsymbol{Y}$ is the observation matrix (identified natural frequencies) and $\hat{\boldsymbol{Y}}$ is the $n \times N$ matrix of independently estimated modal frequencies by means of statistical models. In normal conditions, the matrix $\boldsymbol{E}$ contains the residual variance associated to errors in dynamic identification and to un-modelled exogenous phenomena. If damage occurs, it affects matrix $\boldsymbol{Y}$ and it induces changes in the distribution of E. Therefore, the residual error matrix contains the information about damage. It is used to compute the T^2 statistic, which is given by:

$$T^2 = r\left(\bar{\boldsymbol{E}} - \bar{\bar{\boldsymbol{E}}}\right)^T \Sigma^{-1}\left(\bar{\boldsymbol{E}} - \bar{\bar{\boldsymbol{E}}}\right) \tag{2}$$

where r is an integer factor called group averaging size, $\bar{\boldsymbol{E}}$ is the mean of the residuals in the subgroup of the last r observations, $\bar{\bar{\boldsymbol{E}}}$ and $\boldsymbol{\Sigma}$ are the mean values and the covariance matrix of the residuals, respectively, estimated during the so-called training period in which the structure is considered in healthy conditions. The estimated T^2 distances in healthy conditions must be contained between control limits. A value of the statistical distance that is positioned outside those limits is called an outlier. The limits of T^2 are defined by zero and the value corresponding to a cumulative frequency of 95% in the training period, which is referred as upper control limit (UCL). In such a way, there is the 5% of probability to observe an outliner in healthy conditions. On the contrary, this probability is greater than 5% if damage occurs. Refer to Ubertini et al. (2016) for the detailed description of the SHM procedure.

Table 1 Environmental monitoring sensors installed on the bell tower

Sensor name	*Measurement type*	*Location*	*Height [m]*	*Orientation*
T_1	Air temperature	Shaft indoor	14	S
T_2	Surface temperature	Shaft outdoor	24	S
T_3	Surface temperature	Shaft indoor	24	S
T_4	Air temperature	Shaft indoor	24	N
T_5	Air temperature	Belfry outdoor	27	S
T_6	Air temperature	Befry outdoor	27	N
T_7	Air temperature	Cusp indoor	41	S
T_8	Air temperature	Cusp indoor	41	N
H_1	Air humidity	Shaft indoor	14	S
H_2	Air humidity	Belfry outdoor	27	S

Additional sensors installed on the bell tower consist of two thermocouples connected to the data acquisition system, which measure the temperature every 30 minutes, several standalone sensors model Tinytag by Gemini Data Loggers, namely eight temperature sensors (six dry bulb sensors and two surface sensors), and two humidity sensors. They are placed in several positions, inside and outside the tower, and are used to study the influence of environmental parameters on the natural frequencies. In August 2018, the Tinytag sensors were removed. The list of the environmental sensors installed on the bell tower is given in Table 1.

4 Structural health assessment

4.1 Structural response under seismic excitation and structural health assessment strategy

In the period from 24th August 2016 to 18th January 2017, a series of earthquakes hit Central Italy causing human losses and damage to the built environment. The main shocks within the aforementioned period are displayed in Table 2. Ground motion records for these earthquakes have been obtained from the data provided by the Italian Strong Motion Network (RAN) of the Department of Civil Protection (DPC) and by the Italian Seismic Network (RSN) of the National Institute of Geophysics and Volcanology (INGV), that manage several accelerometric stations deployed all over the country (Pacor et al., 2011; Gorini et al., 2010). Peak values of accelerations at the top of the monument during the seismic events are shown in Table 3. Channels 1, 2 and 3 refer to accelerometers 1, 2 and 3, respectively. For the sake of better understanding the effects of seismic excitations on the bell tower, accelerations due to swinging bells and a strong windstorm are also provided. Root mean square (RMS) values of accelerations in normal conditions are given as well. The measured dynamic response on top of the bell tower in terms of acceleration in the two perpendicular horizontal directions is illustrated in Figure 4. The seismic accelerations are compatible with earthquakes with return periods lower than 30 years, according to the elastic response spectra at the site of the bell tower, which is prescribed by the Italian building code (NTC18, 2018). Detailed analysis of the structural response of the bell tower to the main shocks occurred in 2016 seismic sequence can be found in Ubertini et al. (2018).

Commonly in Italy, expert technicians are asked to evaluate the state of both heritage and ordinary constructions after an earthquake. This first assessment is based on the visual analysis of the damage pattern, which is a characteristic of each structural type. As for heritage buildings, since masonry is the typical material, the assessment is focused on the identification of the kinematic mechanisms which are activated by the earthquake and on the estimation of their severity. Therefore, damage is assessed only when it is accessible and identifiable by the inspectors. In the case of San Pietro bell tower, no damage was clearly recognisable by visual inspections. The presence of the SHM system allowed to support the evaluation of the structural health of the monument and to study the effects of the seismic events based on:

1 the analysis of the output from the novelty analysis, on which the SHM procedure is based

2 the analysis of the correlation coefficients between environmental factors and natural frequencies.

The environmental datasets used in this work concern sensors T_2, T_3, T_5, T_7, T_8. Besides, an AVT was carried out to better characterise the mode shapes of the bell tower. The results of these investigations are described in the next sections.

Table 2 Main earthquakes that interested San Pietro bell tower in the period 24th August 2016–18th January 2017

Epicentre	*Date*	*Mw*	*Distance [km]*	*PGAE [cm/s²]*	*PGAN [cm/s²]*	*PGAZ [cm/s²]*
Accumoli	24th August 2016	6.0	80	915.97	445.59	399.94
Norcia	24th August 2016	5.4	65	176.77	199.76	135.01
Castel. sul Nera	26th October 2016	5.4	65	793.14	373.06	434.10
Ussita	26th October 2016	5.9	65	553.54	420.07	489.29
Norcia	30th October 2016	6.5	65	478.45	634.00	649.74
Pieve Torina	3rd November 2016	4.8	55	235.15	296.08	195.24
Montereale	18th January 2017	5.3	95	195.39	361.17	124.24
Capitignano	18th January 2017	5.4	95	442.64	566.15	188.35
Cag. Amiterno	18th January 2017	5.1	100	272.61	284.87	101.74

Notes: The approximate distance between the monument and the epicentre of the seismic events is reported, together with peak ground accelerations in E-W, N-S and vertical directions (namely PGAE, PGAN, and PGAZ, respectively).

Table 3 Comparison between accelerations recorded on the bell tower in terms of maximum value and RMS (reported in brackets) under different types of excitation, namely: during the most significative episode of the 2016–2017 Central Italy seismic sequence; the swinging of bells on 5th June 2016; the wind storm occurred from 4th March to 6th March 2015; and in normal everyday conditions (only RMS)

Seismic events	*Channel 1 [cm/s²]*	*Channel 2 [cm/s²]*	*Channel 3 [cm/s²]*	*Resultant 1–2 [cm/s²]*
Accumoli	58.61 (9.22)	76.32 (11.09)	79.48 (11.28)	91.40 (14.42)
Norcia	23.52 (3.51)	19.30 (2.81)	18.27 (2.84)	25.37 (4.50)
Castel. sul Nera	37.76 (5.44)	42.36 (4.63)	33.01 (4.60)	42.41 (7.14)
Ussita	60.65 (8.10)	37.81 (4.91)	30.08 (4.72)	64.45 (9.47)
Norcia	94.23 (15.96)	76.27 (10.18)	64.87 (10.08)	94.69 (18.93)
Pieve Torina	5.97 (0.79)	8.18 (0.93)	6.53 (0.89)	8.33 (1.22)
Montereale	16.02 (2.62)	21.61 (2.25)	16.33 (2.28)	21.66 (3.45)
Capitignano	17.19(1.92)	16.35 (2.63)	16.04 (2.69)	17.77 (3.25)
Cag. Amiterno	11.04 (1.63)	16.04 (1.76)	12.05 (1.78)	16.30 (2.40)
Bells	3.39 (1.14)	2.78 (0.87)	2.69 (0.84)	3.51 (1.43)
Wind storm	2.49 (0.11)	4.47 (0.09)	2.42 (0.09)	7.19 (0.19)
Nor. conditions	(0.02)	(0.02)	(0.02)	(0.02)

Figure 4 Measured dynamic response on top of the bell tower in terms of acceleration during the main shocks of the 2016–2017 Central Italy seismic sequence, (a) Accumoli (b) Norcia on 24th August 2016 (c) Castelsantangelo sul Nera (d) Ussita on 26th October 2016 (e) Norcia on 30th October 2016 (f) Pieve Torina on 3rd November 2016 (g) Montereale (h) Capitignano (i) Cagnano Amiterno on 18th January 2017 (see online version for colours)

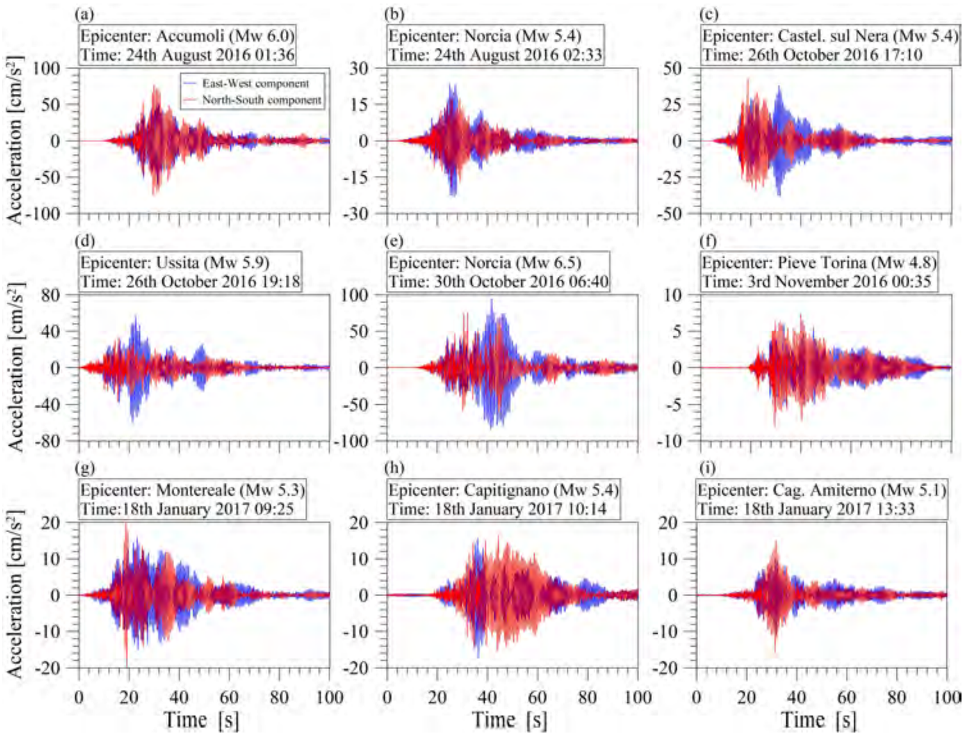

4.2 SHM response

As explained in Section 3, the first step of the SHM procedure is the estimation of the natural frequencies of the monumental bell tower. This operation is performed automatically by means of an SSI technique at intervals of 30 minutes. Five frequencies f_{x1}, f_{y1}, f_{t1}, f_{y2}, and f_{y3} were tracked, corresponding to a bending mode in x-direction (φ_{x1}), one bending mode in y-direction (φ_{y1}), one torsional mode (φ_{t1}) and two higher order bending modes in y-direction (φ_{y2}, ϕ_{y3}), respectively. The time histories of identified natural frequencies presented in Figure 5 cover a period of more than four years. This is a unique case of long-term dynamic SHM for a heritage structure, as far as the authors' knowledge is concerned. The careful examination of the plots of frequencies over time leads to some observations. First, natural frequencies exhibit daily and seasonal fluctuations. In the following section, it will be demonstrated that these shifts are mainly attributable to the effects of temperature variations. Second, a sharp increase in the magnitude of all frequencies is noticed during freezing conditions. In fact, the formation of ice in the micropores of masonry is responsible for the amplification of the material stiffness. The last natural frequency presents a small sharp increase during the last days of October 2017 (highlighted in light grey colour), which is not associated to freezing conditions. It can be a result of tracking uncertainties, probably due to an exchange of f_{y3} and f_{x3} closely spaced frequencies. Given the limited number of sensors in the monitoring system (only three), this may be plausible for a higher order mode. However, this aspect has not been reflected in the control chart (Figure 7) demonstrating to some extent its robustness against uncertainties. Third, a general drop in the magnitude of natural frequencies follows the occurrence of earthquakes. This phenomenon, highlighted in Figure 6, can be linked to the occurrence of structural damages. However, these results include environmental and operational effects. It is noted that the SHM system was not active from August 2018 to January 2019 due to a lightning that struck the tower and ruined the SHM hardware.

Table 4 Information on T^2 statistic data before, during, and after 2016–2017 Central Italy earthquakes: percentage of outliers, mean, and standard deviation

Period	*10th December 2014–23rd August 2016*	*24th August 2016–25th October 2016*	*30th October 2016–17th January 2017*	*18th January 2017–30th April 2019*
% Outliers	5.27	70.05	59.80	45.20
Mean	7.92	26.73	40.67	21.87
St. deviation	8.35	13.65	74.61	26.48

Note: The UCL is 19.58.

Figure 5 Continuously identified natural frequencies of the bell tower (see online version for colours)

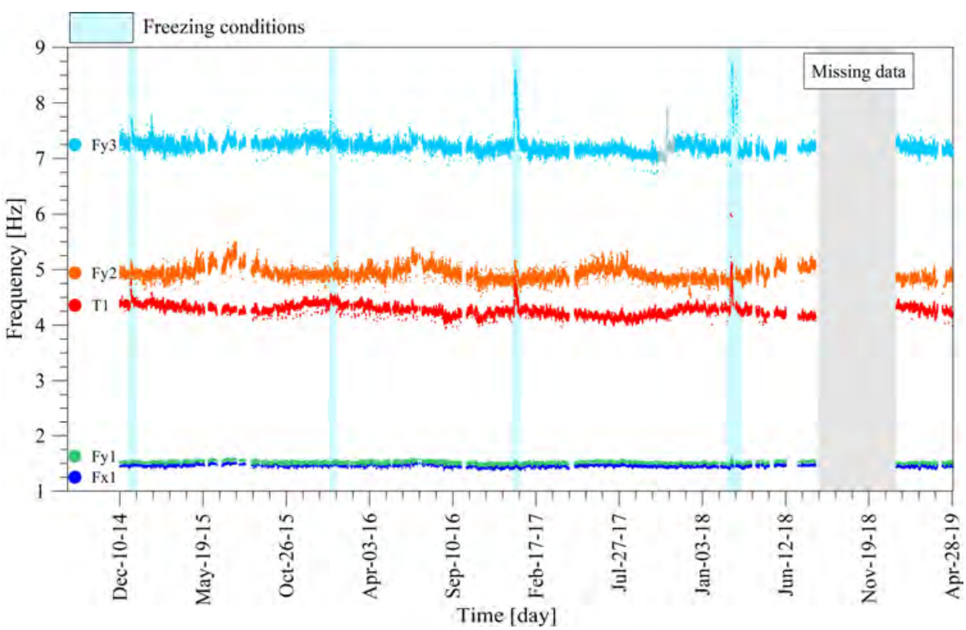

Notes: The periods corresponding to temperatures under 0°C are highlighted in light blue.

Table 5 Comparison between average natural frequencies in pre- and post-earthquake conditions

	$f_{i,average}$ *[Hz]*		*Δf [%]*	σ_i		*Δσ [%]*
	Before	*After*		*Before*	*After*	
f_{x1}	1.468	1.450	–1.2	0.019	0.017	–7.8
f_{y1}	1.533	1.514	–1.2	0.019	0.018	–6.7
f_{t1}	4.330	4.228	–2.4	0.067	0.093	37.4
f_{y2}	4.970	4.900	–1.4	0.108	0.104	–3.6
f_{y3}	7.263	7.176	–1.2	0.077	0.105	36.0

Notes: Δ*f* and Δ*σ* indicates the percentage variation of frequencies and standard deviations, respectively. The reference periods before and after the events are 10th December 2014–23rd August 2016 and 19th January 2017–30th April 2019.

Figure 6 Continuously identified natural frequencies of the bell tower: focus on 24th August 2016 and on 26th and 30th October 2016 (see online version for colours)

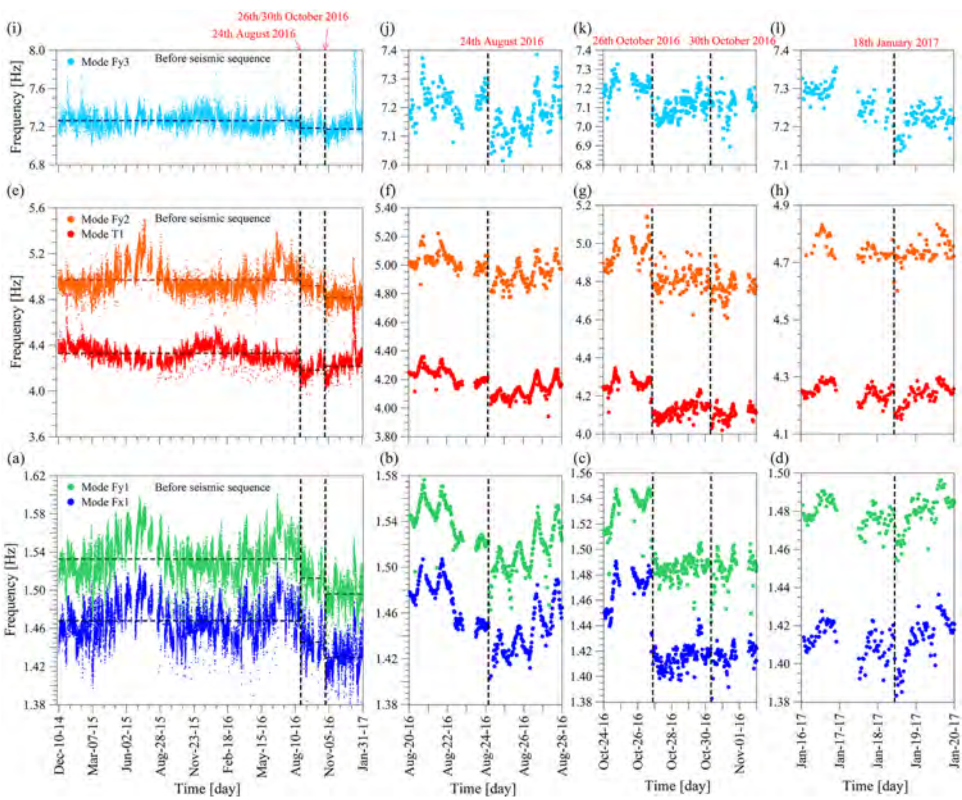

A more objective indication of anomalies is obtained by analysing the control chart provided by the SHM system installed on the bell tower, which is displayed in Figure 7. In addition, the average values, the standard deviations and the percentages of outliers of the T^2 distance before, during, and after the earthquakes are shown in Table 4. The percentage of outliers before 24th August 2016 is roughly 5%: this value denotes that the bell tower is in healthy conditions. After the first seismic event, the percentage of outliers increases significantly. This indicates that the monument is affected by permanent structural damage. The relative frequency histograms of T^2 statistic values before and after the earthquakes are displayed in Figure 8. The probability distribution associated to the T^2 data is clearly non-normal. The plot allows to visualise that after the seismic sequence not only the average value of T^2 distance increases, but also the dispersion of data (the blue histogram is shifted on the right and appears flatter and longer).

Figure 7 Control chart (see online version for colours)

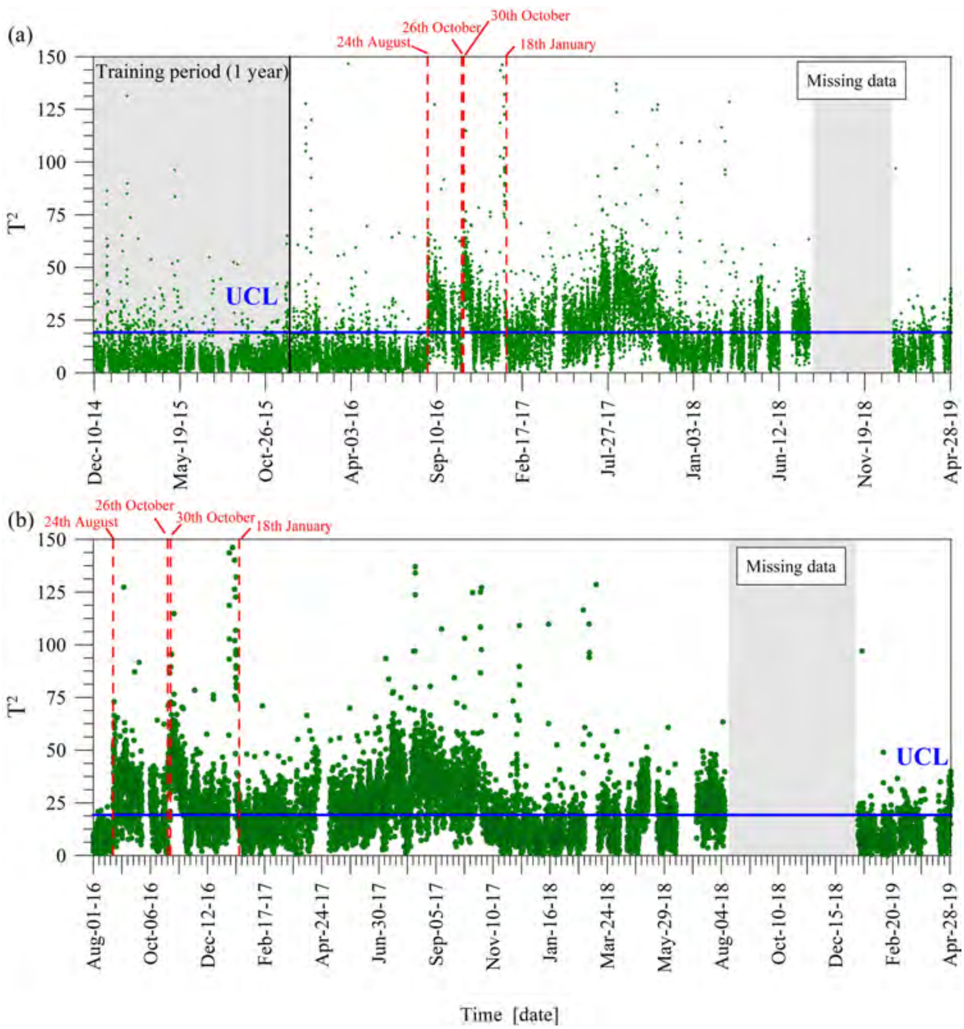

A further confirmation of the effects of the earthquakes is provided by the analysis of the statistics of the long-term frequency data before and after the seismic events occurring in the period 24th August 2016–18th January 2017. The mean values and the standard deviations of the natural frequencies in pre- and post-earthquake condition are provided in Table 5. All the mean values decrease, especially that associated to the torsional mode. The major variations in the moduli of the standard deviations are associated with frequencies f_{t1} and f_{y3}. It follows that φ_{t1} and φ_{y3} are the modes that suffered the most from structural damage.

Figure 8 Relative frequency histograms of T^2 data before and after the earthquakes (see online version for colours)

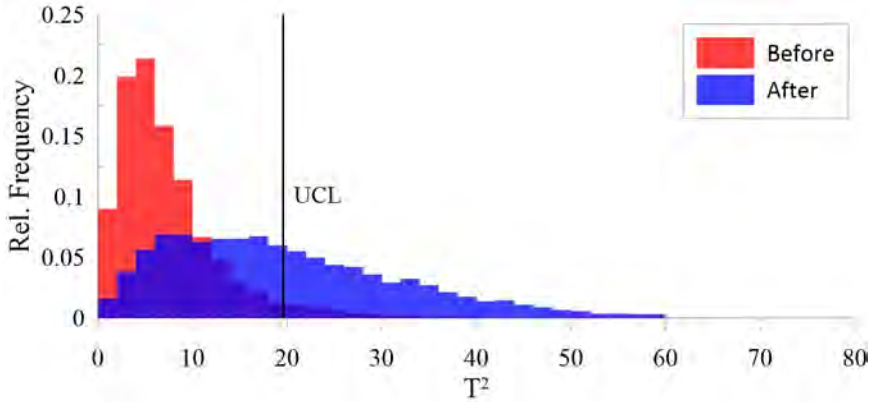

Note: The reference periods before and after the seismic events are 10th December 2014–23rd October 2016 and 19th January 2017–30th April 2019, respectively.

4.3 Correlation analysis

The correlation coefficient r_{xy} is a measure of the strength of the linear relationship between two observed datasets. It is defined as the ratio between the sample covariance σ_{xy} and the sample standard deviations of the two individual datasets σ_x and σ_y. This statistical measure is included in the interval ±1. Values close to +1 and −1 indicate strong positive and negative linear relation between variables, respectively. Values close to zero denote poor linear relation. The correlation coefficients between temperature data and monitoring variables, namely natural frequencies and T^2 statistic, in pre- and post-earthquake conditions are shown in Table 6. The couples of frequencies and temperature datasets showing the highest correlation coefficients are displayed in Figure 9. Data are fitted with linear regression lines with equation:

$$f_i = f_{i,0} + \kappa_{i,T} T_{si} \tag{3}$$

where $i = x1, y1, t1, y2, y3$ indicates the mode, si is the number of the temperature sensors presenting the highest correlation with mode i, $f_{i,0}$ is the frequency at 0°C and $\kappa_{i,T}$ are the frequency-temperature sensitivity coefficients. The parameters that define the fitting lines before and after the seismic events are presented in Table 8. Frequencies f_{x1}, f_{y1}, and f_{y2} and temperatures exhibit positive correlation coefficients both before and after the seismic events. The maximum coefficients correspond to sensor T_5, which records air temperature in the belfry and it is exposed to the south. These results are consistent with other studies found in literature and they can be explained with the closing of micro-cracks within mortar layers due to the thermal expansion of masonry (Gentile et al., 2016). The frequency associated to the torsional mode φ_{t1} shows always a negative correlation with temperatures, especially with those from sensor T_7. The negative correlation is attributed to the thermally induced loss of tension in fibre reinforcements mounted during the last strengthening works and in the metal tie elements (Ubertini et al., 2017). The last frequency f_{y2} exhibits a clear negative correlation with temperatures only after the series of earthquakes. Before, correlation coefficients were either slightly positive or negative, depending on the temperature dataset. In addition to this, it is noticed that the magnitude of the positive correlation coefficients between frequencies f_{x1}, f_{y1}, and f_{y2} and temperatures are basically stable. Conversely, the magnitude of the negative correlation coefficients between frequencies f_{t1} and f_{y3} and temperatures increase considerably in absolute value with respect to all temperature datasets. This is apparent by closely inspecting Table 7, in which the relative variation between correlation coefficients is given. Once again, the behaviour of modes φ_{t1} and φ_{y3} demonstrate to have been particularly affected by the seismic events. Besides what has been said so far, additional relevant fact is that the correlation coefficients between temperatures and T^2 datasets, which were close to zero or slightly negative before earthquakes, are positive after the events, with values ranging between 0.9 and 0.20. This is due to a poor ability of the statistical models in removing the effects of temperature changes from times series of natural frequencies, which was expected since the statistical models were built in the training, undamaged, period. The positive correlation in post-earthquakes conditions can be visually appreciated in Figure 7, by observing the general increase of the magnitude of T^2 data in summer months.

Table 6 Correlation coefficients between monitoring variables (natural frequencies and T^2 statistic) and temperature datasets

	Before					*After*				
	T_2	T_3	T_5	T_7	T_8	T_2	T_3	T_5	T_7	T_8
f_{x1}	0.67	0.62	*0.70*	0.46	0.47	0.68	0.61	*0.68*	0.52	0.55
f_{y1}	0.72	0.72	*0.78*	0.57	0.57	0.72	0.70	*0.76*	0.61	0.64
f_{t1}	–0.40	–0.66	–0.55	*–0.74*	–0.74	–0.51	–0.80	–0.72	*–0.83*	–0.82
f_{y2}	0.70	0.75	*0.77*	0.64	0.64	0.71	0.75	*0.77*	0.68	0.71
f_{y3}	*0.14*	–0.02	0.05	–0.09	–0.09	–0.09	–0.27	–0.21	*–0.29*	–0.28
T^2	0.01	–0.09	–0.04	*–0.11*	*–0.11*	0.09	0.19	0.14	*0.20*	0.19

Notes: Maximum absolute values in ital. The reference periods before and after the seismic events are 2nd March 2015–23rd August 2016 and 19th January 2017–8th July 2018, respectively.

Table 7 Relative variation (in percentage) between correlation coefficients before and after earthquakes

	T_2	T_3	T_5	T_7	T_8
f_{x1}	2	–1	–3	12	18
f_{y1}	–1	–3	–3	7	12
f_{t1}	27	21	30	12	11
f_{y2}	1	–1	1	7	10
f_{y3}	–167	1668	–502	224	200

Table 8 Parameters of best fitting lines between frequencies and temperature data

fi	Before				After			
	Tsi	$f_{i,0}$ [Hz]	$\kappa_{i,T}$ (mHz/°C)	R^2	*Tsi*	$f_{i,0}$ [Hz]	$\kappa_{i,T}$ (mHz/°C)	R^2
f_{x1}	T_5	1.439	1.9	0.49	T_5	1.429	1.4	0.46
f_{y1}	T_5	1.502	2.1	0.61	T_5	1.490	1.7	0.57
f_{t1}	T_7	4.435	–7.3	0.55	T_7	4.337	7.7	0.69
f_{y2}	T_5	4.782	12.4	0.59	T_5	4.745	10.4	0.60
f_{y3}	T_2	7.240	1.1	0.02	T_7	7.209	–3.0	0.10

Note: R^2 indicates the coefficient of determination.

Figure 9 Plots of frequencies and temperature datasets showing the highest correlation coefficients (see online version for colours)

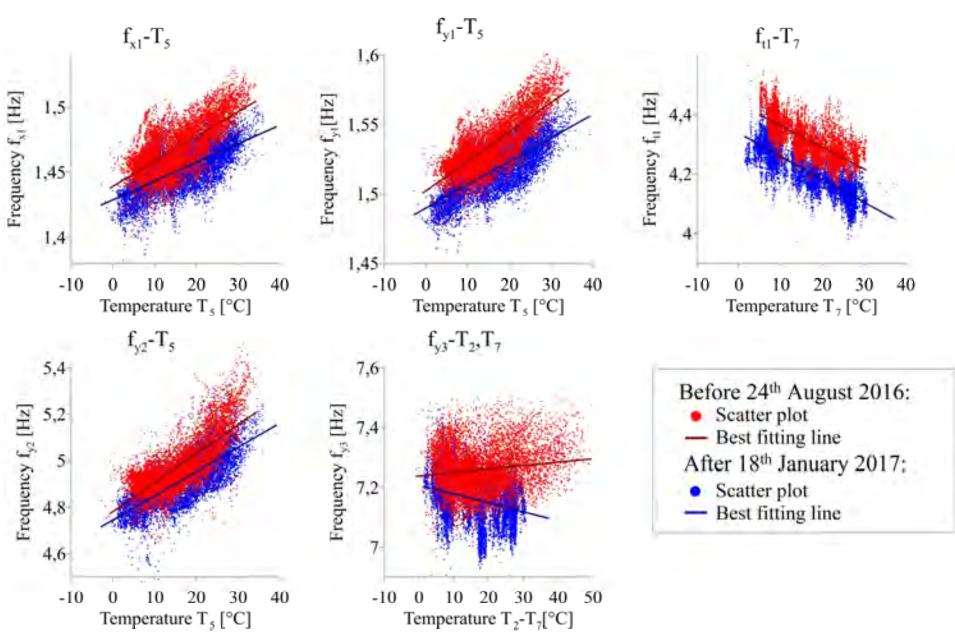

4.4 *Pre- and post-earthquake AVT*

In this section, the results of AVTs performed in pre- and post-earthquake conditions are compared in terms of mode shapes by means of the modal assurance criterion (MAC). The AVT in pre-earthquake conditions was carried out on February 2015 (hence referred as AVT 2015); the AVT in post-earthquake conditions was carried out on May 2017 (hence referred as AVT 2017), see Figure 10. The two AVTs were carried out using several uniaxial piezometric accelerometers, model PCB 393B12, placed at different levels. At each level, three sensors were positioned along the directions X, –Y and Y, respectively. The second accelerometer in Y direction was necessary to detect torsional modes. Data were acquired using a multi-channel system, carrier model cDAQ-9188, with NI 9234 data acquisition modules. Six accelerometers were used during AVT 2015. They were placed at two levels, at the height of 24 m and 40.8 m, respectively. Twelve accelerometers were employed during AVT 2017, namely three sensors per level at the heights of 21 m, 24 m, 26.8 m, and 40.8 m, respectively. However, for the sake of comparison with AVT 2015, here only the sensors placed at 24 m and 40.8 m are considered. Data are processed using the commercial software ARTeMIS (version 5.3) in which several operational modal analysis (OMA) techniques are available. In this study, the enhanced frequency domain decomposition (EFDD) and the stochastic subspace identification – extended unweighted principal component (SSI-UPCX) are used. The results are considered cross-validated when the same modes are identified by both identification techniques.

Figure 10 AVT 2017, (a) localisation of uniaxial accelerometers in the tower (same as AVT 2015) (b) accelerometers in X- and Y-direction (c) accelerometer in Y-direction (d) personal computer connected to the acquisition system (e) data acquisition system and cables (see online version for colours)

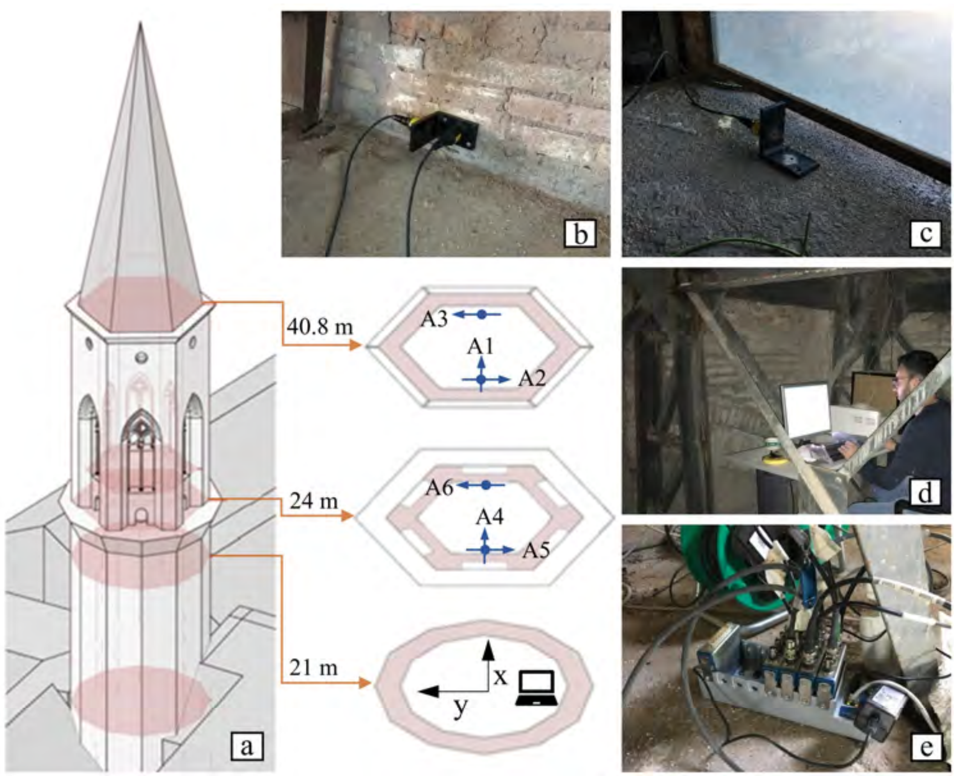

Five vibration modes were clearly identified in both AVT 2015 and AVT 2017: two bending modes in X and Y directions (φ_{x1} and φ_{y1}, respectively), the torsional mode φ_{t1}, and other two bending modes in composed X-Y directions (φ_{xy1} and φ_{xy2}, respectively), see Figure 11. Natural frequencies and MAC coefficients obtained from the two AVTs are summarised in Table 9. The mode shapes obtained with the two different identification techniques are consistent since the MAC values are close to the unity, see Figure 11. The five vibration modes correspond to the natural frequencies continuously identified and tracked by the SHM system installed on the monumental tower. In fact, although the last two modes are referred to as bending in the Y direction, they also have a component in the X direction. The analysis of MAC results highlights substantial variations in the mode shapes of the higher modes (φ_{xy1} and φ_{xy2}) in post-earthquake conditions. However, from the frequency monitoring (Subsection 4.2), the most sensitive modes appear to be the third and the fifth. This discrepancy may be due to the fact that, unlike low frequency modes which are associated with the global dynamic behaviour of the structure, high-frequency modes feature more inflexion points (nodal points), thereby being more sensitive to the effects of local phenomena, such as structural damage (Masciotta et al., 2017b). Moreover, as discussed before, frequency shifts in masonry structures can be associated with factors other than damage, such as temperature fluctuations. Thus, the sole comparison in terms of frequencies is not significant to the end of the identification of structural damages because of the presence of exogenous effects.

Figure 11 Mode shapes identified during AVT 2015 and AVT 2017 (see online version for colours)

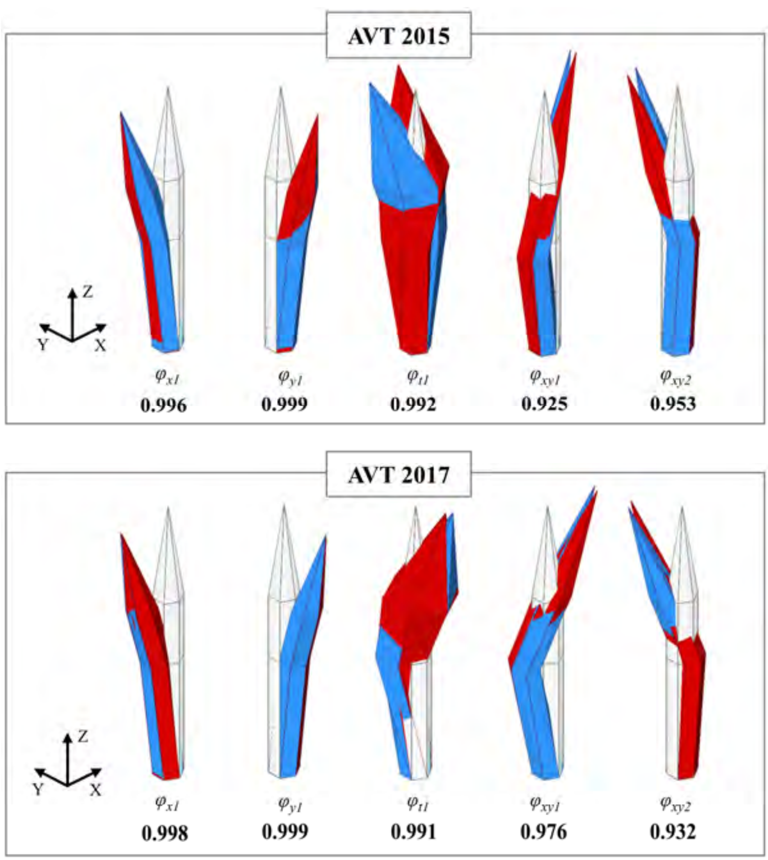

Notes: Undeformed structure in white, EFDD estimator in red, SSI-UPCX estimator in blue. The MAC values between mode shapes from different estimators are reported below the related mode shape.

Table 9 Frequencies and MAC values between identified modes

Mode type	*EFDD – fi [Hz]*		*MAC*	*SSI-UPCX – fi [Hz]*		*MAC*
	AVT 2015	*AVT 2017*		*AVT 2015*	*AVT 2017*	
φ_{x1}	1.45	1.46	0.999	1.45	1.46	0.993
φ_{y1}	1.52	1.53	0.999	1.52	1.53	0.997
φ_{t1}	4.35	4.17	0.982	4.33	4.18	0.993
φ_{xy1}	4.58	4.99	0.848	4.73	4.92	0.857
φ_{xy2}	7.25	7.10	0.841	7.24	7.16	0.652

Figure 12 Re-calibrated control chart (see online version for colours)

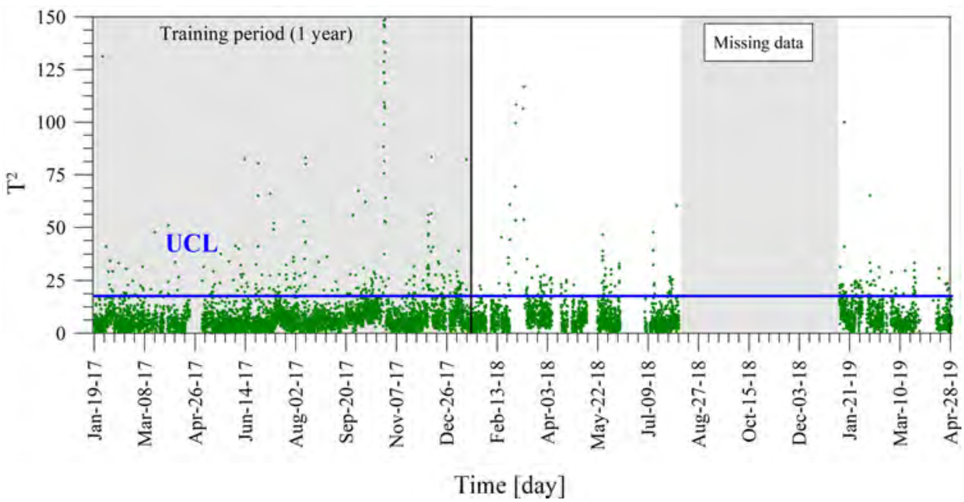

5 Long-term analysis of permanent earthquake-induced effects

In the period from 24th August 2016 to 18th January 2017, the bell tower underwent progressive damages due to important earthquakes, which were recorded by the SHM system. The analysis of the long-term data highlighted that the dynamic characteristics of the monuments and the correlation between natural frequencies and temperature datasets have changed slightly. Thus, it seems appropriate to re-calibrate the SHM system to make it consistent with the new structure under investigation. This is possible thanks to the big amount of available monitoring data after January 2017. The re-calibrated control chart is shown in Figure 12. The considered training period is one year, from January 2017 to January 2018. By the visual analysis of the new control chart with respect to the old one, it is observed that most data are placed under the UCL and that the increase in T^2 magnitude in the summer months has disappeared. In fact, the percentage of outliers after 18th January 2017 is 5.38% and the corresponding UCL is 17.68. Besides, the correlation coefficients between T^2 statistic and temperature datasets T_2, T_3, T_5, T^7, and T_8, are –0.02, –0.02, –0.06, –0.05, and –0.06, respectively. The re-calibration of the control chart has practically eliminated the linear dependence between T^2 data and temperatures, as statistical models relating natural frequencies to temperature data have been re-calibrated. The stability of the outliers under the UCL also indicates that the damage suffered by the tower is not degenerating. Furthermore, the re-calibration of the control chart will enable to detect the occurrence of further structural anomalies in a very objective way.

6 Conclusions

The effects of the 2016–2017 Central Italy seismic sequence on San Pietro bell tower, in Perugia, have been explored in this paper based on four years of SHM data, among which two years covered the pre-earthquake conditions and two years covered the post-earthquake ones. Although the epicentres of the most relevant seismic events were located at a distance between 55 and 100 km, the accelerations recorded by the sensors installed on the monument are of greater intensity up to three orders of magnitude compared to those expected in normal conditions due to the action of traffic and wind. Structural damage clearly attributable to the effect of earthquakes could not be identified by a visual analysis of the monument. However, the occurrence of structural anomalies was confirmed by the analysis of:

1 the output of the SHM algorithm, i.e., the control chart

2 the correlation between natural frequencies and environmental factors

3 the comparison between AVT results before and after the earthquake sequences.

The analysis of the control chart has highlighted percentage of outliers before the beginning of the seismic sequence close to 5%, indicating the general healthy state of the monument. After the first earthquake, the percentage of outliers increased considerably. In addition to this, the mean value of each natural frequency decreases after the earthquakes in a reference time of almost two years. The correlation analysis between temperature and natural frequencies before and after the seismic events highlighted variations in the linear relationship between datasets in terms of correlation coefficients and parameters of best fitting linear regression lines. Regarding AVTs, the analysis of MAC coefficients highlights relevant variations in the mode shapes of higher modes in post-earthquake conditions, which is consistent with previous numerical analyses highlighting the occurrence of slight earthquake-induced damage in the belfry, on the upper part of the structure. Thanks to the big amount of available data, the control chart has been re-calibrated after the seismic events considering a training period of one year. In this way, it is demonstrated that the damage suffered by the tower is permanent and stable. The re-calibration of the SHM algorithm will allow a better identification of possible future damages.

Topics that deserve additional investigations are:

1 the increase in magnitude of the negative correlation between frequencies f_{t1}–f_{y3} and temperatures

2 the onset of positive correlation between T^2 data and temperatures in damaged conditions.

References

Bartoli, G., Betti, M., Facchini, L. and Orlando, M. (2012) 'Non-destructive characterization of stone columns by dynamic test: application to the lower colonnade of the Dome of the Siena Cathedral', *Engineering Structures*, Vol. 45, pp.519–535.

Cabboi, A., Gentile, C., Guidobaldi, M. and Saisi, M. (2015) 'Continuous dynamic monitoring of historic masonry towers using few accelerometers: methodological aspects and typical results', *7th International Conference on Structural Health Monitoring of Intelligent Infrastructures*, Turin.

Cavalagli, N., Comanducci, G., Gentile, C., Guidobaldi, M., Saisi, A. and Ubertini, F. (2017) 'Detecting earthquake-induced damage in historic masonry towers using continuously monitored dynamic response-only data', *Procedia Engineering*, Vol. 199, pp.3416–3421.

Clementi, F. et al. (2017) 'Numerical model upgrading of a historical masonry building damaged during the 2016 Italian earthquakes: the case study of the Podestà palace in Montelupone (Italy)', *Journal of Civil Structural Health Monitoring*, Vol. 7, No. 5, pp.703–717.

De Stefano, A., Matta, E. and Clemente, P. (2016) 'Structural health monitoring of historical heritage in Italy: some relevant experiences', *Journal of Civil Structural Health Monitoring*, Vol. 6, No. 1, pp.83–106.

Elyamani, A., Caselles, O., Roca, P. and Clapes, J. (2017) 'Dynamic investigation of a large historical cathedral', *Structural Control and Health Monitoring*, Vol. 24, No. 3, p.e1885.

Gattulli, V., Lepidi, M. and Potenza, F. (2016) 'Dynamic testing and health monitoring of historic and modern civil structures in Italy', *Structural Monitoring and Maintenance*, Vol. 3, No. 1, pp.71–90.

Gentile, C., Guidobaldi, M. and Saisi, A. (2016) 'One-year dynamic monitoring of a historic tower: damage detection under changing environment', *Meccanica*, Vol. 51, No. 11, pp.2873–2889.

Giordano, P.F., Ubertini, F., Cavalagli, N., Kita, A., Ramos, L.R. and Masciotta, M.G. (2018) 'Diagnostic investigations and structural health state assessment of San Pietro bell tower in Perugia', *10th IMC – Proceedings of the 10th International Masonry Conference*, Milan, Italy.

Gorini, A., Nicoletti, M., Marsan, P., Bianconi, R., De Nardis, R., Filippi, L., Marcucci, S., Palma, F. and Zambonelli, E. (2010) 'The Italian strong motion network', *Bulletin of Earthquake Engineering*, Vol. 8, No. 5, pp.1075–1090.

Guidobaldi, M. (2016) *Vibration-Based Structural Health Monitoring For Historic Masonry Towers*, PhD thesis, Politecnico di Milano, Milano, Italy.

ICOMOS/ISCARSAH (2005) *Recommendations for the Analysis*, Conservation and Structural Restoration of Architectural Heritage.

Kita, A., Cavalagli, N., Comanducci, G. and Ubertini, F. (2017) 'Dynamic testing and monitoring of historic towers for seismic damage detection', *COMPDYN 2017 – Proceedings of the 6th International Conference on Computational Methods in Structural Dynamics and Earthquake Engineering*, Vol. 1, pp.2564–2577.

Lorenzoni, F., Casarin, F., Caldon, M., Islami, K. and Modena, C. (2016) 'Uncertainty quantification in structural health monitoring: applications on cultural heritage buildings', *Mechanical Systems and Signal Processing*, Vols. 66–67, pp.268–281.

Magalhães, F., Cunha, A. and Caetano, E. (2012) 'Vibration based structural health monitoring of an arch bridge: from automated OMA to damage detection', *Mechanical Systems and Signal Processing*, Vol. 28, pp.212–228.

Masciotta, M.G., Ramos, L.F. and Lourenço, P.B. (2017a) 'The importance of structural monitoring as a diagnosis and control tool in the restoration process of heritage structures: a case-study in Portugal', *Journal of Cultural Heritage*, Vol. 27, pp.36–47.

Masciotta, M.G., Ramos, L.F., Lourenço, P.B. and Vasta, M. (2017b) 'Damage identification and seismic vulnerability assessment of a historic masonry chimney', *Annals of Geophysics*, Vol. 60, No. 4, p.S0442.

NTC18 (2018) *Norme Tecniche per le Costruzioni (in Italian)*, Italian Ministry of Infrastructures and Transport.

Pacor, F., Paolucci, R., Luzi, L., Sabetta, F., Spinelli, A., Gorini, A., Nicoletti, M., Marcucci, S., Filippi, L. and Dolce, M. (2011) 'Overview of the Italian strong motion database ITACA 1.0', *Bulletin of Earthquake Engineering*, Vol. 9, No. 6, pp.1723–1739.

Peeters, B., Maeck, J. and De Roeck, G. (2001) 'Vibration-based damage detection in civil engineering: excitation sources and temperature effects', *Smart Materials and Structures*, Vol. 10, No. 3, pp.518–527.

Ramos, L.F., Marques, L., Lourenço, P.B., De Roeck, G., Campos-Costa, A. and Roque, J. (2010) 'Monitoring historical masonry structures with operation modal analysis: two case studies', *Mechanical Systems and Signal Processing*, July, Vol. 24, pp.1291–1305.

Saisi, A., Gentile, C. and Guidobaldi, M. (2015) 'Post-earthquake continuous dynamic monitoring of the Gabbia Tower in Mantua, Italy', *Construction and Building Materials*, 15 April, Vol. 81, pp.101–112.

Ubertini, F., Cavalagli, N., Kita, A. and Comanducci, G. (2018) 'Assessment of a monumental masonry bell-tower after 2016 Central Italy seismic sequence by long-term SHM', *Bull Earthquake Eng*., Vol. 16, No. 2, pp.775–801.

Ubertini, F., Comanducci, G. and Cavalagli, N. (2016) 'Vibration-based structural health monitoring of a historic bell-tower using output-only measurements and multivariate statistical analysis', *Structural Health Monitoring*, Vol. 15, No. 4, pp.438–457.

Ubertini, F., Comanducci, G., Cavalagli, N., Pisello, A.L., Materazzi, A.L. and Cotana, F. (2017) 'Environmental effects on natural frequencies of the San Pietro bell tower in Perugia, Italy, and their removal for structural performance assessment', *Mechanical Systems and Signal Processing*, Vol. 82, pp.307–322.

Ubertini, F., Gentile, C. and Materazzi, A.L. (2013) 'Automated modal identification in operational conditions and its application to bridges', *Engineering Structures*, Vol. 46, pp.264–278.

Worden, K., Sohn, H. and Farrar, C. (2002) 'Novelty detection in a changing environment: regression and interpolation approaches', *Journal of Sound and Vibration*, Vol. 258, No. 4, pp.741–761.